Optimal Vehicle Use in the Presence of Episodic Mobile-Source Air Pollution

Arthur J. Caplan*

Department of Applied Economics

Utah State University

Ramjee Acharya

Department of Applied Economics

Utah State University

July 15, 2019

Abstract

This paper develops a conceptual model of vehicle trips in a region plagued by weather-dependent, mobile-source air pollution, and numerically estimates optimal trips for one of the nation's perennially worst air quality regions in terms of short-term particulate matter. Based upon data-driven parameters and damage estimates, our numerical model generates optimal values for region-wide vehicle trips and associated $PM_{2.5}$ concentrations along with their corresponding time paths. Our dataset includes a host of pertinent weather variables that determine $PM_{2.5}$ concentrations both independently as well as interacted with vehicle trips. As a result, our empirical model enables us to isolate the conditions under which vehicle travel most affects air pollution levels. Our results suggest that maximizing net social welfare in the presence of mobile-source pollution requires substantial reductions in traditional, emissions-generating vehicle usage on days experiencing critical weather conditions – in the case of our study area, temperature inversions. Because they are socially optimal and targeted solely for days with temperature inversions, the estimated reductions in vehicle usage are substantially larger than those proposed by Moscardini and Caplan (2017) to attain the daily National Ambient Air Quality Standard (NAAQS) for particulate matter on an average basis. We find that the optimal reduction in vehicle trips result in corresponding particulate matter concentrations that are roughly six to 13 percent of the NAAQS.

JEL: D62, Q53, Q58

Keywords: optimal vehicle trips; mobile-source air pollution; trip-weather interactions

1 Introduction

Mobile-source air pollutants have proven themselves intractable problems for several of the world's metropolitan areas, particularly in Central and South America (Gallego et al., 2013a,b; Zhang et al., 2016), China (Chen et al., 2013), and the US (ALA, 2017), although as pointed out by Karagulian et al. (2015) the problem is by no means confined to these regions of the world. Ninety percent of the world's population currently resides in locations where local air pollution levels exceed the World Health Organization's (WHO's) ambient standards (WHO, 2017). An estimated 6.5 million premature deaths occur annually due to elevated air pollution concentrations, roughly half of which are attributable to elevated particulate matter ($PM_{2.5}$) concentrations (Apte et al., 2015). The annual mortality rate in the US alone due to elevated air pollution concentrations is estimated to be 200,000, a quarter of which is attributable to vehicle emissions (Caiazzo et al., 2013).

Despite notable achievements made in the control of vehicular emissions during the past 50 years, $PM_{2.5}$ and ground-level ozone concentrations in several US metropolitan areas continue to exceed National Ambient Air Quality Standards (NAAQS) (Acharya and Caplan, 2018b). These exceedances are persistent, episodic, and in certain instances dramatic (Bachmann, 2007; EPHCP, 2017; USEPA, 2017; ALA, 2017). An apparent dichotomy between the pace of technological advancement in controlling mobile-source emissions and the prevalence of localized air pollution problems suggests that in those locations currently contending with unhealthy air quality, technological advancement, e.g., through conversion of a given location's vehicle fleet to a substantial percentage of hybrid and electric vehicles (EVs), is not occurring quickly enough (GAM, 2016; IEDC, 2013). As a result, public policies providing a mixture of incentives are needed to (1) motivate behavioral changes in how households utilize their vehicle fleets, and (2) generate the revenue necessary to fund public investments in technologies capable of hastening more immediate mitigation of the pollution problem.

Recently, market- and non-market-based policies to indirectly control mobile-source emissions have been explored in the literature. Cropper et al. (2014) investigate the use of a permit scheme to control ground-level ozone concentrations in Washington, DC, while Moscardini and Caplan (2017) assess the merits of a seasonal gas tax to control $PM_{2.5}$ concentrations in northern Utah – an area of the country persistently ranked among the worst for short-term particulate concentrations (ALA, 2017).[1] A host of studies have similarly investigated the effectiveness of both voluntary and mandatory driving restrictions on controlling vehicle emissions. For example, Henry and Gordon (2003), Cummings and Walker (2000), and Cutter and Neidell (2009) assess the impact of voluntary driv-

---

[1] Studies assessing the efficacy of congestion pricing, or tolls, are indirectly related to issue of controlling mobile-source pollution via a market-based instrument (c.f., Button and Verhoef, 1998; Phang and Toh, 2004; Anas and Lindsey, 2011).

ing restrictions in the US, while Zhang et al. (2016), Gallego et al. (2013a,b), and Osakwe (2010) investigate the efficacy of mandatory restrictions in South America.

The question of which tax/subsidy policy mix most closely mimics what would otherwise be a first-best (Pigovian) emissions tax on mobile-source emissions is addressed in a series of studies using national, household-level data on vehicle choice and usage. In the case of homogeneous households (in terms of income and preferences over different automobile characteristics), Fullerton and West (2002) find that a Pigovian tax on emissions by itself would induce households to optimally choose vehicle miles traveled (VMT), engine size, fuel type, and pollution control equipment (PCE).[2] Alternatively, "complicated" gas and vehicle taxes can attain the same result – the complication stemming from (1) the taxes needing to depend upon specific vehicle characteristics (which would have to be determined at the pump in the case of a gas tax, e.g., via a "smart pump" that could conceivably adjust an individual motorist's gas tax according to the vehicle's VMT, engine size, fuel type, or PCE), and (2) the households needing to be informed as to how their vehicle characteristics affect the tax rate(s), both of which carry heavy informational burdens for the regulator and the households. A combination of separate fixed (i.e., uncomplicated) tax rates also induces socially optimal household choices – a result similar to those reported in the earlier studies of Eskeland (1994), Innes (1996), Harrington et al. (1998), and Sevigny (1998).

When households instead express heterogeneous preferences over vehicle characteristics, Fullerton and West (2002) find that the uniform Pigouvian emissions tax rate determined in the case of homogeneous households also works – a result driven by the uniformity of emissions in their model.[3] However, all other types of taxes must be household-specific as opposed to solely vehicle-characteristic specific. The authors further investigate how far second-best uniform tax rates deviate from the first-best, individualized rates. They find that second-best optimal tax rates on engine size and gasoline depend upon the elasticities of demand for these goods, as well as the correlation between preferences for VMT and engine size.[4]

---

[2]Fullerton and West (2010) extend their 2002 model by including vehicle age as an additional characteristic upon which to levy a tax or subsidy. The authors solve numerically for second-best, uniform tax rates and find that 71 percent of the gain from the emissions tax can be achieved by a combination of uniform tax rates levied on gasoline, engine size, and vehicle age. A gasoline tax alone attains 62 percent of the Pigovian gain. If the additional administrative costs of implementing an emissions tax are greater than 0.07 percent of the sum of all affected individuals' incomes, then the three-part instrument may dominate the Pigovian tax. West and Williams III (2005) compare the costs of a gasoline tax and corporate average fuel economy (CAFE) standards taking into account interactions with preexisting tax distortions. The authors find that the interactions reduce the cost of the gasoline tax but increase the cost of CAFE standards, thus expanding the cost advantage enjoyed by the gasoline tax.

[3]We thank an anonymous referee for pointing out that this type of result carries over to congestion pricing when the marginal cost of congestion is likewise uniform across agents (Arnott and Kraus, 1998).

[4]Bento et al. (2009) extend Fullerton and West (2002) by investigating the extent to which increases in a gasoline tax motivate changes in household-level vehicle fleet composition and VMT in a general-equilibrium model linking markets for new, used, and scrapped vehicles and accounting for heterogeneity in household characteristics. The authors find that each cent-per-gallon increase in the price of gasoline reduces equilibrium gasoline consumption by roughly 0.2 percent. Taking into account revenue recycling, the impact of a 25-cent gasoline tax on the average household is estimated to be approximately $30 per year (2001 dollars). Distributional impacts depend importantly on how additional revenues from the tax increase are recycled, e.g., in proportion to household-income or VMT, or via flat (equal-proportion) revenue recycling.

Absent from this literature is a dynamic framework within which to estimate optimal vehicle usage on a regional basis – in particular the extent to which aggregate vehicle usage should be curtailed during weather-induced episodes of elevated (and accumulated) mobile-source air pollution. Notwithstanding the issue of whether gasoline or vehicle taxes or permits are the instrument(s) of choice, the central question we seek to answer in this study is how regional authorities might best establish targeted reduction levels in vehicle usage that are tailored to episodic "outbreaks" of air pollution events (known in our study area as "red air day" episodes), particularly when household- and vehicle-level data are unavailable. Instead, daily measures of region-wide vehicle usage, pertinent weather conditions, and actual pollutant concentrations are readily obtainable for both empirical and numerical estimation.

To demonstrate how this question can be answered we calibrate a simple model of accumulating pollutants with a unique dataset consisting of daily, region-specific weather variables, vehicle trip counts, and $PM_{2.5}$ concentration readings from one of the nation's perennially worst air quality regions, Northern Utah (the region's short-term particulate matter problem is discussed at greater length in Section 3). Included in the calibration exercise are damage estimates obtained from the US Environmental Protection Agency's (USEPA's) recently released Environmental Benefits Mapping and Analysis Program (BenMAP) (USEPA, 2018) and benefit estimates (associated with vehicle usage) based on data obtained from a host of relevant sources.

We find that dramatic reductions in emissions-generating vehicle trips should be targeted for temperature inversions that occur sporadically in Northern Utah during the winter months, and that correlate closely with red air day episodes. Because they are socially optimal and targeted solely for days with temperature inversions, the estimated reductions in vehicle usage are markedly larger than those proposed for Northern Utah by Moscardini and Caplan (2017) to attain the USEPA's daily NAAQS of 35 $\mu g/m^3$ on an average basis. Concomitantly, we find that optimal reductions in vehicle trips result in $PM_{2.5}$ concentrations that are roughly six to 13 percent of the NAAQS. As expected, the time path for daily trip counts during temperature inversions exhibits a steep decline from its initial level, thus reaching its optimal level rather quickly. The corresponding stock of $PM_{2.5}$ decreases less abruptly, reaching its optimal level in roughly double the amount of time.

The next section develops the conceptual model underpinning our subsequent empirical and numerical analyses presented in Section 4. Section 3 briefly describes the study area for our empirical and numerical analyses. Section 5 concludes the paper.

2 The Conceptual Model

Following Phaneuf and Requate (2017, Chapter 13), let period t's instantaneous, or marginal, change in regional $PM_{2.5}$ concentrations be expressed as,

$$\dot{S}_t = f(E_t, S_t; W_t) \tag{1}$$

where E_t represents aggregate vehicle emissions during period t, S_t denotes the stock of $PM_{2.5}$ concentrations at the beginning of period t, and W_t indicates a vector of prevailing weather conditions.[5] Assume $f(\cdot)$ is increasing in E_t, decreasing in S_t, and either increasing or decreasing in W_t depending upon the specific weather variable in question. Vehicle emissions are in turn a function of aggregate vehicle usage, which in our case is represented by region-wide vehicle trips, T_t, e.g., $E_t = g(T_t; W_t)$, $\frac{\partial E_t}{\partial T_t} = g'(T_t; W_t) > 0$, $g(0; W_t) = 0$.[6] Thus, (1) can be re-expressed as,

$$\dot{S}_t = h(T_t, S_t; W_t) \tag{2}$$

with $h(\cdot)$ increasing in T_t.

The region's decision problem is expressed as,

$$\max_{T_t} \quad \int_{t=0}^{\infty} (B(T_t) - D(S_t)) e^{-rt} dt$$
$$\text{subject to} \quad \dot{S}_t = h(T_t, S_t; W_t), S_0 > 0$$

where benefit function $B(T_t)$ is assumed increasing and strictly quasi-concave in T_t, damage function $D(S_t)$ is increasing and convex in S_t, $r > 0$ is a standard discount rate, and e denotes Euler's number. Except where necessary, we henceforth drop the subscript t designation.

Including a discount rate in the modeling context of what is effectively both a seasonal and episodic problem accounts for the persistence of health costs through time associated with contemporaneous elevations in $PM_{2.5}$ concentrations that occur during red air day episodes (c.f. Pope, 1989; Broome et al., 2015; USEPA, 2016). Because the health costs associated with any given red air day episode are incurred throughout what can be a lifetime for some victims, the need for discounting these future costs is evident.

---

[5]Note that an additional parameter could be added to function $f(\cdot)$ accounting for background emissions, e.g., from stationary sources. However, in the context of our model stationary-source emissions are considered exogenous, either because regulations targeting these emissions are already in force, mobile- and stationary-source emissions are determined independently from one-another, or mobile-source emissions make the predominant contribution. Our model is therefore tailored to regions of the world where one or more of these exogeneity conditions are met.

[6]In regions where vehicle usage is not the sole contributor, but is nevertheless the predominant anthropogenic source of pollution concentrations, the latter condition can be expressed as $g(0; W_t) \approx 0$.

We lose no generality in modeling the decision problem as occurring over an infinite time horizon, whether that horizon covers (1) a predetermined series of finite-period winter seasons, (2) an undetermined series of temperature-inversion periods within a given season, or (3) a given temperature-inversion period of undetermined length within a given season (Chiang, 1992). For this study we adopt the latter of these three time-horizon perspectives. Specifically, we assume the region is initially in a steady state facing neither a temperature inversion nor an elevation in $PM_{2.5}$ concentrations (i.e., concentrations are low and $\dot{S} = 0$). The region then enters a temperature-inversion period of undetermined length with concomitant rising concentrations (i.e., $\dot{S} > 0$). The key question addressed in this paper is, in the midst of a temperature inversion what is the optimal adjustment in vehicle trips, T, to return the region to its initial steady state? We consider the temperature inversion as presenting the regional authority with a continuum of incremental decision points stretching over a time horizon with an unknown terminal point that itself stretches to infinity in the limit.[7]

The associated current-value (conditional) Hamiltonian function for the region's problem is expressed as,

$$\mathcal{H}(T, S, \lambda; W) = B(T) - D(S) - \lambda(h(T, S; W))$$ (3)

with λ serving as the problem's Lagrange multiplier.[8] In the context of our problem, λ represents the marginal impact of an additional concentration unit of $PM_{2.5}$ (measured in micrograms per cubic meter, $\mu g/m^3$) on optimal net benefit in a given period.

For consistency with our empirical model in Section 4.1, we re-express (2) in linear form,

$$\dot{S}_t = \beta_1 T + \beta_2 S + \beta_3 \cdot (T \cdot W) + \beta_4 \cdot (S \cdot W),$$ (4)

where β_1 and β_2 represent the coefficient estimates of region-wide vehicle trip's and the stock of $PM_{2.5}$'s effects on marginal $PM_{2.5}$ concentrations, respectively. Vectors β_3 and β_4 represent the respective sets of coefficient estimates that measure the effects of interactions between pertinent weather variables and both vehicle trips and the stock of $PM_{2.5}$. Coalescing the β coefficients into $\beta_T = \beta_1 + \beta_3 \cdot \bar{W} > 0$ and $\beta_S = \beta_2 + \beta_4 \cdot \bar{W} < 0$, with $\bar{W}$ representing the weather variables measured at their respective central, or expected, values the problem's (interior) optimality conditions can be expressed as,

$$B'(T) - \lambda \beta_T = 0$$ (5)

$$\dot{\lambda} + r\lambda = D'(S) + \lambda \beta_S.$$ (6)

---

[7] As Chiang (1992) points out, extending the time horizon to infinity creates a more comprehensive optimization framework.
[8] The Hamiltonian is conditional on weather conditions.

Note that (5) implies $\lambda > 0$. In a steady state, where $\dot{\lambda} = 0$, equation (6) implies $\beta_S - r < 0$.[9],[10]

Lastly the problem's transversality condition is expressed as,

$$\lim_{t \to \infty} \lambda_t S_t e^{-rt} = 0. \tag{7}$$

Consistent with the interpretations of β_T and β_S, we assume (7) is satisfied at $\bar{W}$.

In a steady state, optimality conditions (5) and (6) solve for,

$$B'(T^*) = -\frac{\beta_T D'(S^*)}{\beta_S - r}. \tag{8}$$

where the $*$ superscript henceforth denotes optimal values. Along with (5), equation (8) can be used to determine comparative static effects associated with the equilibrium, coalesced here in Proposition 1.

Proposition 1. *Optimal vehicle trips and the stock of $PM_{2.5}$ both increase in r, and vehicle trips decrease in β_T and β_S. The remaining comparative statics effects are indeterminate.*

Proof. See Appendix A.

From Proposition 1 we see that the optimal levels of T, and thus S, respond positively to an increase in the discount rate. An increased discount rate makes private vehicle travel in the current instant relatively more valuable. This is due to the fact that health costs incurred in future periods – which are nevertheless associated with current pollution levels – are discounted more heavily, thus providing greater incentive for households to travel in that instant. To the contrary, increases in the effects of both vehicle travel and the stock of $PM_{2.5}$ on marginal $PM_{2.5}$ concentrations (i.e., respective increases in β_T and β_S) raise the social cost of vehicle travel, thus reducing T^* (recall that $\beta_S < 0$, thus an increase represents a smaller negative effect). Ultimately, the 'cross-partial' effects of β_T on S^* and β_S on S^* are indeterminate. The former effect depends upon the difference between the rate at which the marginal benefit of vehicle trips diminishes, $B''(T^*)$, and the marginal damage associated with the stock of $PM_{2.5}$, $D'(S^*)$; the latter upon the difference between $B''(T^*)$ and the marginal benefit of vehicle trips, $B'(T^*)$ (see equations (A.4) and (A.6) in Appendix A).

---

[9]Note that $r - \beta_S > 0$ can be interpreted as a risk-adjusted discount rate, where the adjustment accounts for environmental risk premium $-\beta_S > 0$

[10]As shown in Section 4.1, we adhere to the hierarchical ordering principle (c.f., Li et al., 2006 and Hamada and Wu, 1992) in empirically estimating (4) by including the vector term $\beta_5 \cdot W$, which controls for independent weather-related effects on marginal $PM_{2.5}$ concentrations, $\dot{S}$, and ensures more precise measurement of the model's key interaction terms. Because weather conditions affect marginal $PM_{2.5}$ concentrations solely when interacted with vehicle trips and lagged stock of $PM_{2.5}$, we do not account for the independent weather effects in our numerical analysis of Section 4.3. Also, by conditioning our estimates of β_T and β_S on the weather variables' respective expected values, $\bar{W}$, we are per force deriving expected-value, or ex ante outcomes. An alternative approach would be to parameterize functions $B(\cdot)$ and $D(\cdot)$ on $\bar{W}$ directly. However, we have no evidence to suggest that this is in fact germane to the problem at hand.

Referring to equation (4) and the corresponding expressions for β_T and β_S, the optimal time path for S is defined as,

$$\dot{S} = \beta_T T + \beta_S S. \tag{9}$$

To find T's optimal time path we differentiate (5) with respect to time t and combine this result with (5) and (6), resulting in,

$$\dot{T} = \frac{\beta_T D'(S) + B'(T)(\beta_S - r)}{B''(T)}. \tag{10}$$

Together, equations (9) and (10) determine how optimal vehicle trips and the stock of $PM_{2.5}$ evolve jointly over time, starting from any initial stock of $PM_{2.5}$, S_0. Whether the evolution converges to a steady-state equilibrium of course depends upon the underlying dynamics of the system defined by these two equations.

Setting $\dot{S} = \dot{T} = 0$ in equations (9) and (10), we can derive the corresponding isoclines and depict the steady-state equilibrium (conditioned on $\bar{W}$) in a standard phase diagram. The diagram is presented in Figure 1 (the derivation of which is provided in Appendix B).

[INSERT FIGURE 1 HERE]

The results in Appendix B also lead to Proposition 2 concerning the equilibrium's local and global stability properties.

Proposition 2. *The conditional steady-state equilibrium is either locally stable or a convergent fluctuation. The equilibrium is also asymptotically globally stable for strictly convex damages (i.e., $D''(S) > 0$) and small-enough discount rate r.*

Proof. See Appendix B.

Thus, S_0 evolves to (T^*, S^*) from any S_0 located in a local neighborhood of the equilibrium, and from any neighborhood – near or far – for a small-enough discount rate. In concert with joint evolution of T and S to the steady-state equilibrium, the optimal feedback strategy for vehicle trips, denoted $T = T(S)$, can be shown to solve as the ordinary differential equation (see Appendix C),

$$T'(S) = \frac{\beta_T D'(S) + B'(T(S))(\beta_S - r)}{B''(T(S))(\beta_T T(S) + \beta_S S)}, \tag{11}$$

which, given the nonlinearity of $B(T(S))$, is itself highly nonlinear and complicated. In the numerical analysis to follow we therefore eschew deriving the closed-form solution for this equation, and instead rely on calculating the joint evolution of (9) and (10) in order to derive the optimal time paths of T and S directly. Nevertheless, we

can see from (11) that optimal vehicle trips respond negatively to the stock of $PM_{2.5}$ for (1) large-enough marginal impacts of vehicle trips on marginal $PM_{2.5}$ concentrations (β_T), (2) large-enough marginal damages ($D'(S)$), (3) small-enough marginal benefits from vehicle trips ($B'(T(S))$), and/or (4) a small-enough net impact of the stock of $PM_{2.5}$ on marginal $PM_{2.5}$ concentrations ($\beta_S - r$).

In transitioning to the numerical analysis in Section 4.3, we henceforth assume that $D(S) = dS$ and $B(T) = b\sqrt{T}$, $d > 0, b > 0$. For comparison purposes we also conduct numerical analysis using an alternative form of the social benefit function, $B(T) = b\ln(T)$ and report results in Appendix D. Using readily available data, we are able to calibrate the value of b in the benefit function. As we discuss in Section 4.2, Moscardini and Caplan (2017) and Acharya and Caplan (2018a) provide evidence for a linear damage function in our particular study area; evidence that permits a specific estimate of constant d.[11]

From equations (5), (6), and (9), our numerical expressions for optimal vehicle trips, the stock of $PM_{2.5}$, and multiplier λ, respectively, are

$$T^* = \left(\frac{b(\beta_S - r)}{2\beta_T d} \right)^2 \tag{12}$$

$$S^* = -\frac{b^2(\beta_S - r)^2}{4d^2\beta_T\beta_S} \tag{13}$$

$$\lambda^* = -\frac{d}{\beta_S - r}, \tag{14}$$

and from equation (10) we obtain,

$$\dot{T} = -\frac{4d\beta_T T^{\frac{3}{2}} + 2b(\beta_S - r)T}{b}. \tag{15}$$

Equations (9) and (12)–(15) are used in Section 4.3 to derive our key numerical results.

3   The Study Area

Elevated $PM_{2.5}$ concentrations are a persistent, episodic pollution problem in Northern Utah's Cache County – Cache County is the portion of the purple highlighted area in Figure 2 located beneath the state boundary with Franklin County, Idaho.[12] As elaborated on in Moscardini and Caplan (2017) and Acharya and Caplan (2018a), the stock of $PM_{2.5}$ frequently spikes well above the USEPA's National Ambient Air Quality Standard (NAAQS)

---

[11]We note that under the assumption of linear damages Proposition 2 no longer holds for global stability, since the Brock and Scheinkman (1976) positive definiteness test conducted in Appendix B no longer applies.

[12]The collection of highlighted areas in this map depict what is commonly known as Utah's Wasatch Front. This region experiences some of the nation's highest $PM_{2.5}$ concentrations during what is known as the winter inversion season. As a result, the region has been in persistent nonattainment of the USEPA's National Ambient Air Quality Standard.

of 35 $\mu g/m^3$ averaged over any 24-hour period during the winter months (primarily December - February).[13] For example, Figure 3 depicts annual distributions of PM2.5 concentrations in the region during the 2002 - 2007 period (the period 2008 - 2012 depicts similar annual distributions). Clearly, the stock of $PM_{2.5}$ frequently spikes above the 24-hour NAAQS (horizontal red line) during the winter months (primarily December - February), creating red air day episodes. The figure also reveals the variability in spikes from year to year. For instance, during the 2002, 2004, and 2005 inversion seasons spikes occurred more frequently, reaching markedly higher levels than those experienced in the 2003, 2006, and 2007 inversion seasons.

[INSERT FIGURES 2 AND 3 HERE]

Annually averaged $PM_{2.5}$ concentrations for Northern Utah during our study period (2002–2012) are 26.69, 13.9, 35.63, 27.0, 13.77, 14.3, 16.84, 21.75, 21.78, 17.63, and 8.04, respectively, as compared with the USEPA's annual primary and secondary NAAQS for $PM_{2.5}$ concentrations of 12 and 15 $\mu g/m^3$. Further, we note that the recent alternative standard set in Utah's State Implementation Plan (SIP) for areas in non-attainment with the 24-hour NAAQS of 35 $\mu g/m^3$ – calculated as an average of three running three-year averages of 98th percentile concentration levels surrounding the baseline year 2010 (known as the "baseline design value") – is set at 40.7 $\mu g/m^3$ for Cache County (UAQB, 2014). This new standard therefore effectively raises the 24-hour standard by over five $\mu g/m^3$ relative to the long-standing threshold of 35 $\mu g/m^3$. By way of comparison, the World Health Organization's (WHO's) guidelines for annual and daily $PM_{2.5}$ concentrations are set at 10 and 25 $\mu g/m^3$, respectively (WHO, 2006). Hence, applied on a seasonal basis (which is necessary in our study area given the seasonal nature of the problem), annually averaged concentrations often exceed (sometimes considerably) both the WHO and USEPA annual standards. Northern Utah's concentrations also frequently exceed the WHO and USEPA daily standards.

Table 1 provides information on the extent of Northern Utah's red air day problem during our study period, and its coincidence with temperature inversions. Wintertime temperature inversions occur as the temperature at ground level falls beneath the temperature at higher elevations, trapping pollutants at the surface (UDEQ, 2016b). As elevation rises temperature gradually decreases. Given conducive barometric-pressure, snowfall, snow depth, and wind-speed conditions, descending warm air creates an inversion layer. The inversion layer traps $PM_{2.5}$ concentrations between geologic barriers which, in the case of Northern Utah, are the Wellsville and Bear River Mountain Ranges (see Wang et al (2015) and Malek et al (2006) for further discussion of the temperature-inversion phenomenon).

---

[13]As shown in Section 4.1, the conditional mean value of daily $PM_{2.5}$ concentrations during the winter months – conditional on the existence of a temperature inversion – rises to just over 37 $\mu g/m^3$ in northern Utah during our study period, illustrating the positive relationship between temperature inversions and elevated $PM_{2.5}$ concentrations.

[INSERT TABLE 1 HERE]

As shown in Table 1, the number of red air day episodes (RADEs) and their average lengths vary randomly over the years of our study, showing no clear upward or downward trends over time. The number of these episodes range from zero in 2012 to eight in 2005, with an average of just over four episodes per year. The average lengths of the episodes similarly range from zero to roughly eight days. A similar pattern unfolds for temperature inversion events (TIEs), with the average number of inversion events per year reaching 5.5 and the average length reaching 3.5 days. The table's final column provides a static assessment of the coincidence between increases in $PM_{2.5}$ concentrations ($\dot{S} > 0$) and the presence of a temperature inversion. The relative frequency with which the two coincide on an annual basis ranges from just over nine percent in 2012 to over 40 percent in 2005, providing unconditional evidence of the extent to which temperature inversions coincide with red air day episodes. Figure 4 depicts a specific coincidence between the formation of a red air day episode and a temperature inversion event experienced in Northern Utah during the month of January 2004. The emergence, prolongation, and subsidence of the red air day episode closely tracked a corresponding temperature inversion over the course of 23 consecutive days.

[INSERT FIGURE 4 HERE]

Short-term exposure to elevated $PM_{2.5}$ concentrations is linked to increased respiratory problems in humans, such as asthma attacks, as well as increased respiratory symptoms, such as coughing, wheezing and shortness of breath. Long-term exposure can cause premature death due to heart and cardiovascular disease associated with heart attacks and strokes. Some studies suggest that long-term exposure can cause cancer as well as harmful developmental and reproductive defects, such as infant mortality and low birth weight (USEPA, 2016; Dockery et. al, 1993; Pope et. al, 1995; Pope, 1989).

Together with agricultural and industrial processes, vehicle emissions contribute a predominant share of $PM_{2.5}$ concentrations in Northern Utah (UAQB, 2014). During a typical winter temperature inversion, anywhere from 60 to 85 percent of all $PM_{2.5}$ is created by secondary particulate formation (UDEQ, 2016a; Moscardini and Caplan, 2017). Secondary particulate formation occurs when precursor emissions of nitrogen oxides (NOx), sulfur oxides (SOx), and especially volatile organic compounds (VOCs) from vehicle emissions react and combine in the atmosphere to create stocks of $PM_{2.5}$ (UDEQ, 2016a). According to the Utah Department of Environmental Quality (UDEQ), VOCs are highly reactive. As they break apart they combine with other gaseous chemicals to form nitrates. These nitrates then react with ammonia to form ammonium nitrate, the leading contributor to $PM_{2.5}$ concentrations in the region. The UDEQ has therefore concluded that reducing vehicle VOC emissions offers the best

approach to reducing the regions $PM_{2.5}$ concentrations during winter temperature inversions (UDEQ, 2016a). In what follows, we empirically estimate the extent to which these weather conditions interact with Northern Utah's vehicle usage and accumulated $PM_{2.5}$ concentrations in determining the rate at which the concentration levels change over time.

4 Empirical and Numerical Results

4.1 Regression Analysis

We begin this section with a discussion of the regression model(s) used to estimate the set of beta coefficients included in (4), presented in condensed form in (9) as β_T and β_S, as well as the corresponding empirical results. The data for our regressions are compiled from several different sources; each variable in the dataset consisting of a daily time step for the years 2002–2012. Since the problem addressed in this study occurs seasonally (from December–February) we restrict the dataset to these three months each year. The stock of $PM_{2.5}$ is recorded hourly for Cache County by the Utah Division of Air Quality (UDAQ) at EPA station code 490050004 located in downtown Logan (UDEQ 2016).[14] The weather variables – consisting of temperature gradient, wind speed, humidity, atmospheric pressure, snow depth, and snowfall level – were obtained from the Weather Underground and the Utah Climate Center (Weather Underground, 2016; Utah Climate Center, 2016). Lastly, vehicle trip count data was obtained from the Utah Department of Transportation (UDOT, 2014). The Automatic Traffic Recorder (ATR) stations for the trip count data in Cache County are #303, #363, and #510, which cover the county's main north-south transportation artery (see Moscardini and Caplan (2017) for further background on the ATR stations).

Specific variable names and summary statistics are presented in Table 2. Of particular note are the mean values for (unconditional) daily $PM_{2.5}$ stock levels, daily $PM_{2.5}$ concentrations conditional upon the existence of a temperature inversion ($TEMP > 0$), trip counts, (unconditional) temperature gradient, and temperature gradient conditional on the existence of a temperature inversion. On average, the daily stock of $PM_{2.5}$ exceeded 18 $\mu g/m^3$ during our study period. As expected, the conditional mean value of daily $PM_{2.5}$ concentrations – conditional on the existence of a temperature inversion – rises to just over 37 $\mu g/m^3$, illustrating the positive relationship between temperature inversions and elevated $PM_{2.5}$ concentrations in our study area.[15]

[INSERT TABLE 2 HERE]

---

[14]Station 490050004 was moved five miles north of downtown Logan to the town of Smithfield shortly after the conclusion of our study period. It is now identified as station 490050007.

[15]The correlation coefficient between S and $TEMP$ is 0.71, which corroborates the close relationship between the two variables.

The average aggregate trip count of roughly 45,000 trips per day is admittedly a lower-bound estimate of actual trips since it represents the sum of trips recorded solely at the county's three ATR stations. However, because the ATR locations remain unchanged during the study period, they nevertheless provide an accurate relative measure of vehicle trips, where in this case "relative" refers to the capturing of daily variation in trips. Daily variation in trips is needed for our regression analyses. Lastly, we note that on average the temperature gradient is negative during our study period, i.e., the average winter day does not experience a temperature inversion. However, on days when a temperature inversion is experienced, the gradient is roughly $9°F$. As we now show, any public policy designed to control $PM_{2.5}$ concentrations in our study area should consider including a specific target for vehicle travel on temperature-inversion days.

Table 3 presents our regression results for two models. Model 1 includes the entire set of weather variables and two- and three-way interaction terms, while Model 2 excludes (un-interacted) $PRESS$ and three-way interaction term $T * HUMWIND * TEMP$ as a result of its (1) high correlation with other included variables, and (2) persistent statistical insignificance in explaining variation in dependent variable $\dot{S}$.[16] Applying Cumby and Huizinga's (1992) Portmanteau test for white noise error structure, we find that including first and second lags of $\dot{S}$ as regressors (denoted $\dot{S}_{t-1}$ and $\dot{S}_{t-2}$, respectively) for the years 2004, 2011, and 2012 satisfies the null hypothesis of no auto-correlation in the residuals. Only a single lag is necessary for the years 2003 and 2006-2010.[17] As the Durbin χ^2 statistics for both models indicate, the overall regressions with these two lagged terms included as regressors are consistent with an absence of second-order autocorrelation in the residuals.[18]

[INSERT TABLE 3 HERE]

As indicated in Table 3, the marginal effect of the (lagged) stock of $PM_{2.5}$ on marginal concentrations is negative, as expected, but statistically insignificant.[19] The marginal effect of $PM_{2.5}$ concentration level is, however, negative and statistically significant when interacted with $HUMWIND$ and $SNOWF$. Vehicle trips exhibits an expected positive effect on marginal concentrations and is statistically significant in Model 2. Trip count is also

[16] To save space in the table, statistically insignificant two- and three-way interaction terms are unreported for both models. As in Moscardini and Caplan (2017), the variable $WIND$ is also excluded from both models given its persistent statistical insignificance. The variable $TEMP$ was likewise dropped from both models due to its persistent statistical insignificance when not interacted with other variables. Following Moscardini and Caplan (2017), we also tested for potential endogeneity in the trip-count variable using a standard Durbin-Wu-Hausman test (Davidson and MacKinnon, 1993). We could not reject the null hypothesis of exogeneity. Results for our alternative specifications and the Durbin-Wu-Hausman test are available from the author upon request.

[17] Data for 2002 was dropped from the analysis due to a preponderance of missing values. Data was also dropped for 2005 since introducing an inordinate number of lags of $\dot{S}$ was necessary to control for potential autocorrelation in that year.

[18] Stata/IC version 14.2 for windows (64-bitx86-64) was used for the regression analysis. Because of inherent gaps in our data – due to our analyzing solely the winter-month data – we were accordingly restricted to applying the Cumby and Huizinga (1992) test year-by-year.

[19] We use S_{t-1} as the regressor rather than S_t in order to account for the $PM_{2.5}$ concentration level measured at the end of the previous day (which proxies as the stock at the beginning of the current day). As pointed out by Moscardini and Caplan (2017, footnote 8), $PM_{2.5}$ in our study area is indeed a cumulative problem, which in turn provides a pretext for including S_{t-1} as a control variable in our regression analysis.

positive and significant when interacted with $TEMP$ and $HUMWIND$ and when included in three-way interactions with $HUMWIND$ and $TEMP$, $SNOWF$ and $TEMP$, and $SNOWD$ and $TEMP$. Vehicle trips have a negative effect on marginal concentrations when interacted with $PRESS$ and included in a three-way interaction with $PRESS$ and $TEMP$. These results therefore suggest that the positive marginal impact of vehicle trips on marginal $PM_{2.5}$ concentrations is enhanced on days experiencing temperature inversions. This impact is enhanced at higher $SNOWD$ and $HUMWIND$ levels. To the contrary, the marginal impact of vehicle trips during temperature inversions is attenuated under higher snowfall and air pressure levels. Together, these results suggest that if policy is able to be "fine-tuned", it should target vehicle trips made on days with temperature inversions, particularly when snow depth and $HUMWIND$ levels are also higher.

Lastly, the negative coefficient on $YEAR$ indicates that, all else equal, marginal $PM_{2.5}$ concentrations in the study area have been falling year by year. Further, similar to Moscardini and Caplan (2017) and Acharya and Caplan (2018a), we find that $HUMWIND$ has a negative effect on marginal concentrations. As in Acharya and Caplan (2018a) the effect of snowfall(snow depth) is negative(positive). Summary statistics for our regressions indicate that roughly 65 percent of the variation in marginal $PM_{2.5}$ concentrations is explained by the models, and the null hypothesis that the estimated coefficients are jointly equal to zero is rejected.

Using the results from Table 3, we are now able to calculate coefficient values for β_T and β_S in equation (9). These estimates are provided in Table 4. Recall from equation (4) that the weather-variable interaction terms incorporated in the calculations of β_T (i.e., β_1 and β_3) and β_S (i.e., β_2 and β_4) are evaluated at their respective mean values (reported in Table 2).[20]

[INSERT TABLE 4 HERE]

4.2   Calculation of Marginal-Benefit and Marginal-Damage Parameters

The two remaining parameters to be estimated for our numerical analysis are the marginal-benefit parameter, b, and marginal-damage parameter, d. To calculate b we first obtained a national estimate of the annual cost of vehicle ownership and operation, which for 2017 is estimated to be roughly $9,000 (AAA, 2017). This value is most likely a lower-bound estimate of the most-recent annual benefit associated with owning and operating a vehicle, particularly in our case, where our ultimate goal is to derive a measure of the benefit per vehicle trip taken during the winter months (when the value of traveling in warmth is presumably higher). We then utilize the Bureau of Labor Statistic's (BLS's) CPI Inflation Calculator to obtain corresponding values for each of the years represented

---

[20]For example, the calculation for β_T from Model 1 equals (roughly) (0.0003 x 8.74) + (2.8e-07 x 249.41) + (3.0e-08 x 249.41 x 8.74) - (1.1e-07 x 14.22 x 8.74) + (3.9e-08 x 123.65 x 8.74) - (9.1e-06 x 30.18 x 8.74). We say "roughly" because the values contained in Table 3 are based on the unrounded coefficient values obtained from the regression analyses, rather than the rounded values presented in Table 3.

in our dataset, resulting in a mean estimate of the annual benefit of owning and operating a vehicle in our study area during our study period of \$7,504.56 (BLS, 2018). Next, we obtained the Utah State Tax Commission estimates of the number of passenger vehicles registered in our study area for each of the years represented in our dataset, resulting in a mean value of 50,288 (USTC, 2018). Multiplying these two values together results in our mean estimate of the aggregate annual benefit of vehicle travel in our study area of \$377,389,090.

To convert this aggregate benefit value into a corresponding measure of benefit per vehicle trip, we calculate the aggregate number of vehicle trips taken annually in our study area. From our dataset we are able to calculate the average number of trips taken per day of the week (Sunday-Saturday), which are then each multiplied by 52 days. Summing these day-of-the-week averages results in an annual average of 16,359,044 vehicle trips, which, when divided into our mean estimate of the aggregate annual value of vehicle trips results in an estimated benefit-per-trip of \$23.07. Next, we multiply our benefit-per-trip estimate by our average number of vehicle trips per day of 45,000 (from Table 2) to obtain our estimated benefit per day of \$1,038,150.[21] Lastly, appealing to our assumed functional relationship $B(T) = b\sqrt{T}$, we obtain our calibrated estimate of $b = 4,894$.

To derive an estimate of d we utilize the relevant health damage estimates for our study area presented in Acharya and Caplan (2018a). As reported in Acharya and Caplan (2018a), The EPA's Environmental Benefits Mapping and Analysis Program (BenMAP) is used to derive these estimates (USEPA, 2018).[22]

Figure 5 depicts the reverse of Acharya and Caplan's (2018a) benefit estimates associated with progressively more reductions in $PM_{2.5}$ concentrations, and thus charts out the corresponding damage function, i.e., the relationship between increasing concentrations (effectively starting from an initial stock level) and the associated damages.

[INSERT FIGURE 5 HERE]

As shown, this relationship is linear. The associated (dotted) trend line's intercept is statistically indistinguishable from zero ($p - value = 0.33$), it's slope is \$4.4 million ($p - value = 0.00$), and adjusted-$R^2 = 0.99$.[23] Dividing \$4.4 million by 90 winter days/year results in $d = \$49,324$.[24]

---

[21]This value is slightly larger than the value of \$1,033,743 obtained by simply dividing \$377,389,090 by 365 days.

[22]Acharya and Caplan (2018a) utilized version 1.1 of the Community Edition of BenMAP to derive their health damage estimates. BenMAP is a Windows-based program using Geographical Information Systems (GIS) to estimate the health benefits and associated economic benefits of changes at a regional scale. To obtain their estimates Acharya and Caplan (2018a) inputted the following parameters for $PM_{2.5}$ concentrations in Cache County, Utah to obtain a "pooled valuation result": (1) monitor rollback (percentage basis) and rollback grid type with monitor library year 2008, (2) percentage rollback of 25 percent, (3) fixed radius of 10 km, (4) US Census – county level for population dataset, 2008, and (5) Pope et al. (2002) health impact functions.

[23]Linear damage functions for mobile-source emissions are also assumed by Fullerton and West (2010) and the earlier studies of Small and Kazimi (1995), Burtraw et al. (1998), McCubbin and Delucchi (1999), and USFHWA (2000), and Parry and Small (2005). Linearity was also assumed in Liu and Yu's (1976) early estimations of generalized average damage functions.

[24]Recall that in our study area elevated $PM_{2.5}$ concentrations present a health risk solely during the three winter months of December-February.

4.3 Numerical Results

Table 5 contains our estimates of the optimal values T^*, S^*, and λ^* for regression models 1 and 2 and assumed social discount rates, $r = \{0.01, 0.03, 0.05, 0.07\}$.[25] These estimates are derived using equations (12) – (14) from Section 2, estimates of parameters β_T and β_S from Section 4.1, and estimates of b and d from Section 4.2. Numerical results for the alternative specification of the social benefit function, $B(T) = b\ln(T)$, are contained in Appendix D.

[INSERT TABLE 5 HERE]

As shown in Table 5, Model 1, optimal daily vehicle trip counts during temperature inversions range between 3,100 at the lowest assumed social discount rate of one percent to 5,000 at the highest rate of seven percent (representing dramatic reductions relative to the daily average of 45,000 trips during our study period). These optimal counts fall further to between 1,700 and 2,800 for Model 2, reflecting Model 2's higher estimated values for β_T and β_S. Concomitant with the benefits of vehicle travel being a likely lower-bound estimate, we consider our corresponding optimal daily trip counts to be lower-bound estimates as well. Achieving trip counts at this low of a level during days with temperature inversions (recall the average daily trip count in our study area is 45,000) would require aggressive action on the part of the region's drivers on those particular days, likely achieved through a variety of means, e.g., voluntary or mandatory driving restrictions, greater use of public mass transit and zero-emission and Tier 3 vehicles, etc.[26]

Results for the corresponding optimal stock of $PM_{2.5}$ on days with temperature inversions are similarly dramatic. The concentrations never exceed five $\mu g/m^3$, even at the higher discount rates (relative to our study period's average $PM_{2.5}$ concentration level during temperature inversions of 37 $\mu g/m^3$). Optimal concentration levels do not exceed 3.5 $\mu g/m^3$ at lower discount rates. The main driver behind the sizable reductions in vehicle trip counts and concentration levels is obviously BenMAP's estimates of the health damages associated with elevated $PM_{2.5}$ concentrations in the study area (as shown in Figure 5). As mentioned in Section 1, our estimates of the socially optimal $PM_{2.5}$ concentration levels are roughly six to 13 percent of the NAAQS for our study period of 35 $\mu g/m^3$). As shown in Table 6 in Appendix D, optimal reductions in vehicle trips and the attendant stock of $PM_{2.5}$ are slightly more dramatic for social benefit function $B(T) = b\ln(T)$. Further, because the divergence in optimal vehicle trips

---

[25]These rates are consistent with those surveyed in Greenstone, et al. (2013) and historically used by OMB (2003) in their benefit-cost analyses.

[26]Relying on the use of zero-emission vehicles would require a transformation far more ambitious than that envisioned by California's recent Zero-Emissions Vehicle (ZEV) Action Plan for that state (CGO, 2016). Recall that while California's plan effectively calls for the replacement of approximately four percent of its statewide vehicle fleet by 2025 (CGO, 2016), if Cache County were to rely solely on the transformation of its fleet to ZEVs the corresponding replacement rate would range from 89 percent to 93 percent using Model 1's results (associated with 3,100 and 5,000 trip counts, respectively) and an even larger replacement rate using Model 2's results.

across Models 1 and 2 is not as pronounced for each discount rate, optimal $PM_{2.5}$ concentration levels are larger for Model 2 than Model 1, unlike the results for social benefit function $B(T) = b\sqrt{T}$.

Figures 6 and 7 present the optimal time paths for vehicle trips and the associated stocks of $PM_{2.5}$, respectively, at the onset of a temperature inversion, assuming an initial state of 25,000 daily vehicle trips and a $PM_{2.5}$ concentration of 10 $\mu g/m^3$ (shown here assuming Model 1's parameter values and a discount rate of three percent).[27]

[INSERT FIGURES 6 AND 7 HERE]

Most notably, the time path for optimal daily trip counts during temperature inversions exhibits a steep decline from its initial level and reaches its steady-state level of approximately 3,700 trips after roughly seven periods.[28] This makes sense because once in a temperature inversion aggregate vehicle trips elevate the stock of $PM_{2.5}$ toward a red air day episode. The most effective and therefore socially optimal way for the region to adjust to the inversion is via a rapid reduction in vehicle trips, especially given the $PM_{2.5}$ stock's attenuated response to these reductions. In practice, enactment of public policies such as mandatory or voluntary driving restrictions and more widespread use of mass transit could conceivably lead to the attainment of the steady-state level of vehicle usage at a faster pace.

The time path for optimal $PM_{2.5}$ concentrations during temperature inversions is smoother. The decline from its initial level is not nearly as steep, reaching the steady state roughly 14 periods later. This lingering response is a consequence of the weather-dependency of vehicle trip's effects on the marginal concentration levels, and the fact that, although statistically significant, the estimated effects are relatively small in magnitude (recall the interaction coefficient estimates for variable T reported in Table 3 and the corresponding β_T values derived in Table 4). Results for social benefit function $B(T) = b\ln(T)$ follow the same pattern – see Figures 8 and 9 in Appendix D.

5 Conclusions

This paper has developed a dynamic framework within which to estimate optimal, steady-state vehicle usage on a regional basis – in particular the extent to which aggregate vehicle usage should be curtailed during weather-induced episodes of elevated (and accumulated) mobile-source air pollution. In this context, we have sought to

---

[27]The vehicle trip path begins to overshoot the optimal trip count at roughly 30,000 daily trips, reflecting the fact that this model simulates optimal rather than current trip counts. Because optimal trip counts are markedly lower than what is currently recorded in our study area, we are not surprised that our numerical model demonstrates this type of volatility when the initial trip count is effectively so distant from what we know is its optimal steady-state value. To avoid introducing this volatility into our model, we therefore assume an initial state that represents more than half of the daily vehicle-trip average of 45,000 and associated $PM_{2.5}$ concentration level during our study period. Results are similar using Model 2's parameter estimates and for each of the remaining discount rates assumed for this study.

[28]For our numerical analysis we delineate the passage of time as a generic "period" rather than "day" in order to maintain consistency with the instantaneous nature of our coneptual model. Thinking of periods as days in no way alters the qualitative character of our results.

answer the question of how regional authorities might best establish target reduction levels in steady-state vehicle usage that are tailored to episodic "outbreaks" of air pollution events, particularly when household- and vehicle-level data are unavailable. Instead, daily measures of regionwide vehicle usage, pertinent weather conditions, and actual pollutant concentrations are readily obtainable for both empirical and numerical estimation.

Toward this end, we have calibrated a simple model of accumulating pollutants using a unique dataset for one of the nation's perennially worst air quality regions, Northern Utah. Included in the calibration exercise are damage estimates obtained from the USEPA's recently released BenMAP (USEPA, 2018) and benefit estimates (associated with vehicle usage) based on data obtained from a host of relevant sources. We find that dramatic reductions in emissions-generating vehicle trips should be targeted for temperature inversion episodes that occur sporadically in Northern Utah during the winter months; episodes leading to elevated $PM_{2.5}$ concentration levels. Because they are socially optimal and targeted solely for days with temperature inversions, the estimated reductions in vehicle usage are markedly larger than those proposed for Northern Utah by Moscardini and Caplan (2017), which are calibrated to attain the daily NAAQS for $PM_{2.5}$ concentrations on an average basis. Corresponding reductions in $PM_{2.5}$ concentration levels are similarly dramatic, ultimately resulting in concentrations that are roughly six to 13 percent of the NAAQS for our study period. Further, we find that the time path for optimal daily trip counts during temperature inversions exhibits a steep decline from its initial level, thus reaching its steady-state level rather quickly. The corresponding stock of $PM_{2.5}$ decreases less abruptly, reaching its steady-state level in roughly double the amount of time due to the weather-dependent and relatively small effects of reduced vehicle trips on marginal concentration levels.

Irrespective of whether the mobile-source pollution problem is weather-dependent (and thus episodic in nature), the approach developed in this paper demonstrates how to jointly estimate socially optimal target, or benchmark, levels for the pollutant and its primary contributing source. In our specific case – elevated $PM_{2.5}$ concentration levels during "red air day" episodes in Northern Utah – the benchmarks are estimated to be starkly below current environmental standards, suggesting that future policies tailored to control these episodes will need to be more aggressive than the vehicle emissions testing and public education programs implemented to date (see Moscardini and Caplan (2017) for further details on these programs). As we have shown in this paper, optimal values for a pollutant and its primary contributing source (along with their associated time paths) are relatively straightforward to estimate, even when the problem is weather-dependent.

Data permitting, the procedures developed in this study are replicable in other regions of the world currently contending with mobile-source pollution problems. This is obviously not to say that household-specific longitudinal data on vehicle usage (e.g., vehicle miles traveled, idling times, etc.) would not greatly improve our ability to

measure the marginal impacts of vehicle usage on $PM_{2.5}$ concentrations in study areas such as northern Utah. Rather, we show that coarser measures of vehicle usage can nevertheless be leveraged effectively. With a socially optimal estimate of vehicle usage in hand, regional authorities will then be able to better target their policies, e.g., vehicle emissions or more complicated gas and vehicle-differentiated taxes, such as those previously explored by Fullerton and West (2002) and Bento et al. (2009). Lastly, it is important to bear in mind the pace with which the composition of a given region's vehicle fleet is changing, e.g., away from traditional combustion-engine to electric vehicles, which all else equal portends reduced effects of vehicle usage on pollutant concentrations over time. The rate at which vehicle trips would then need to be curtailed in an optimal framework – which we have shown to be otherwise quite dramatic – would be concomitantly ameliorated.

Appendices

A Steady-State Comparative Statics Effects

From equations (5) and (8) we obtain

$$\frac{\partial T^*}{\partial r} = \frac{-\beta_S B'(T^*)}{|H|} > 0 \tag{A.1}$$

$$\frac{\partial S^*}{\partial r} = \frac{\beta_T B'(T^*)}{|H|} > 0 \tag{A.2}$$

$$\frac{\partial T^*}{\partial \beta_S} = \frac{\beta_S B'(T^*) - \beta_T D''(S^*) S^*}{|H|} < 0 \tag{A.3}$$

$$\frac{\partial S^*}{\partial \beta_S} = \frac{B''(T^*)(\beta_S - r) S^* - \beta_T B'(T^*)}{|H|} \gtreqless 0 \tag{A.4}$$

$$\frac{\partial T^*}{\partial \beta_T} = \frac{\beta_S D'(S^*) - \beta_T D''(S^*) T^*}{|H|} < 0 \tag{A.5}$$

$$\frac{\partial S^*}{\partial \beta_T} = \frac{B''(T^*)(\beta_S - r) T^* - \beta_T D'(S^*)}{|H|} \gtreqless 0 \tag{A.6}$$

where $|H| = \beta_T{}^2 D''(S^*) - B''(T^*)(\beta_S - r)\beta_S > 0$. Applying the assumed curvature conditions on functions $D(\cdot)$ and $B(\cdot)$, $\beta_S < 0$, $\beta_S - r < 0$, and $\beta_T > 0$, equations (A.1) – (A.6) result in Proposition 1.

B   Stability of the Steady State

Setting $\dot{S} = \dot{T} = 0$ in equations (9) and (10) results in isoclines denoted as,

$$T_T(S) = B'^{-1}\left(-\frac{\beta_T D'(S)}{\beta_S - r}\right) \tag{B.1}$$

$$T_S(S) = -\frac{\beta_S S}{\beta_T} \tag{B.2}$$

where $T_T(S)$ represents the isocline for $\dot{T} = 0$ and $T_S(S)$ similarly represents the isocline for $\dot{S} = 0$. Further, $B'^{-1}(\cdot)$ is the inverse function of $B'(\cdot)$; specifically $B'^{-1}\left(-\frac{\beta_T D'(S)}{\beta_S - r}\right)$ is the inverse of $B'\left(-\frac{\beta_T D'(S)}{\beta_S - r}\right)$. Note that this implies $B'^{-1}(\cdot) > 0$, and that $B'^{-1}(\cdot)$ is itself decreasing in S.

The easiest way to see these two results is via example. Let $B(T) = \sqrt{T}$. Then $B'(T) = \frac{1}{2\sqrt{T}} \implies B'^{-1}(B'(\cdot)) = T = \frac{1}{4B'(\cdot)^2}$. Thus, $B'^{-1}(B'(\cdot)) > 0$ and $B'^{-1}(B'(\cdot))$ is decreasing in $B'(\cdot)$ (i.e., $B'^{-1'}(B'(\cdot)) < 0$). In our case, $B'^{-1}(B'(\cdot)) = B'^{-1}\left(-\frac{\beta_T D'(S)}{\beta_S - r}\right) > 0$, since $-\frac{\beta_T D'(S)}{\beta_S - r} > 0$. Further, given that we assume $B''(T) < 0$, $B'^{-1}\left(-\frac{\beta_T D'(S)}{\beta_S - r}\right)$ is decreasing in S, since, as shown in our example, $B'^{-1}(\cdot)$ evaluates at the reciprocal of its input value.

Equations (B.2) and (B.1) therefore imply,

$$\frac{\partial T_T(S)}{\partial S} < 0 \tag{B.3}$$

$$\frac{\partial T_S(S)}{\partial S} > 0 \tag{B.4}$$

which depicts the isoclines in Figure 1. The corresponding arrows of motion follow directly from (B.1) and (B.2).

Mathematically, the test for local stability stems from the linearized system,

$$\begin{bmatrix} \dot{\lambda} \\ \dot{S} \end{bmatrix} = A \begin{bmatrix} \lambda \\ S \end{bmatrix} + B$$

where, using (5), (6), and (9),

$$A = \begin{bmatrix} (\beta_S - r) & D''(S^*) \\ \beta_T^2 B'^{-1'}(T^*) & \beta_S \end{bmatrix}.$$

Noting $|A| > 0$ and $tr(A) = 2\beta_S - r < 0$ and appealing to Chiang and Wainwright (2005), the system is either a stable node or focus, depending upon $(tr(A))^2 \gtrless 4|A| \implies r \gtrless \sqrt{-4\beta_T^2 B'^{-1'}(T)D''(S^*)}$. To check whether the system's path fluctuates on convergence to the steady state, we need to specify specific functional forms for $B(T)$ and $D(S)$ and check the system's eigenvalues. As mentioned at the end of Section 2, we assume $D(S) = dS$ and

$B(T) = b\sqrt{T}$, $d > 0, b > 0$ for the ensuing numerical analysis in Section 3. Using these specifications, equations (5) and (6) can be re-expressed as,

$$T = \left(\frac{b}{2\lambda\beta_T}\right)^2 \tag{B.5}$$

$$\dot{\lambda} = dS + \lambda(\beta_S - r). \tag{B.6}$$

Substituting (B.5) to (9) results in,

$$\dot{S} = \frac{b^2}{4\lambda^2\beta_T} + \beta_S S. \tag{B.7}$$

Thus,

$$\begin{bmatrix} \dot{\lambda} \\ \dot{S} \end{bmatrix} = A \begin{bmatrix} \lambda \\ S \end{bmatrix} + B$$

where,

$$A = \begin{bmatrix} (\beta_S - r) & 0 \\ -\frac{b^2}{2\lambda^3\beta_T} & \beta_S \end{bmatrix},$$

and

$$B = \begin{bmatrix} 0 \\ 0 \end{bmatrix}.$$

Letting I represent the 2x2 identity matrix, and μ the values for which determinant $|A - \mu I| = 0$, we are able to derive matrix A's associated eigenvalues μ_1 and μ_2, denoted succinctly as $\mu_{1,2}$,

$$\mu_{1,2} = \frac{(\beta_S - r) \pm \sqrt{(\beta_S - r)^2 - 4\beta_S(\beta_S - r)}}{2}. \tag{B.8}$$

Equation (B.8) indicates that $\mu_1 < 0$ and $\mu_2 < 0$ (since $4\beta_S(\beta_S - r) > 0$), confirming the local stability result obtained above. However, we can also see from (B.8) that if $4\beta_S(\beta_S - r) > (\beta_S - r)^2$, then $\mu_{1,2}$ solves as conjugate complex roots, each with negative real parts ($\beta_S - r < 0$), which in turn indicates a convergent fluctuation.

To characterize the system's global stability conditions we appeal to Brock and Scheinkman's (1976) positive definiteness test, where

$$|Q| = \begin{vmatrix} -\frac{\partial^2 \mathcal{H}}{\partial S^2} & \frac{r}{2} \\ \frac{r}{2} & \frac{\partial^2 \mathcal{H}}{\partial \lambda^2} \end{vmatrix} > 0 \tag{B.9}$$

22

implies global stability. Appealing to (3) we see that,

$$\frac{\partial^2 \mathcal{H}}{\partial S^2} = -D''(S) < 0. \tag{B.10}$$

Further, totally differentiating (5) with respect to T and λ results in $\frac{dT}{d\lambda} = \frac{\beta_T}{B''(T)} < 0$. Appealing to the envelop theorem we therefore have,

$$\frac{\partial^2 \mathcal{H}}{\partial \lambda^2} = -\beta_T \frac{dT}{d\lambda} > 0. \tag{B.11}$$

Hence, (B.9)–(B.11) imply global stability for small-enough r.

C   Optimal Feedback Strategy for Vehicle Trips

Differentiating (5) with respect to t results in,

$$\dot{\lambda} = \frac{B''(T) T'(S) \dot{S}}{\beta_T}. \tag{C.1}$$

Using (9) to eliminate $\dot{S}$ in (C.1) we obtain,

$$\dot{\lambda} = \frac{B''(T) T'(S) (\beta_T T + \beta_S S)}{\beta_T}, \tag{C.2}$$

and similarly using (5) and (C.2) to eliminate $\dot{\lambda}$ and λ from (6) results in,

$$\frac{B''(T) T'(S) (\beta_T T + \beta_S S)}{\beta_T} = D'(S) + \frac{B'(T) (\beta_S - r)}{\beta_T}, \tag{C.3}$$

which can be rewritten as equation (11).

D Numerical Results for Social Benefit Function $B(T) = b \ln(T)$

[INSERT TABLE 6 AND FIGURES 8 AND 9 HERE]

References

Acharya, R. and A.J. Caplan (2018a) Optimal investment to control episodic air pollution. Unpublished manuscript, Department of Applied Economics, Utah State University.

Acharya, R. and A.J. Caplan (2018b) Optimal investment to control episodic air pollution: the case of the Wasatch Front, Utah. Unpublished manuscript, Department of Applied Economics, Utah State University.

American Automobile Association (AAA) (2017) Your driving costs. *AAA News Room*. Available on the Internet at https://newsroom.aaa.com/auto/your-driving-costs/.

American Lung Association (ALA) (2017), State of the air. Available on the Internet at http://www.lung.org/our-initiatives/healthy-air/sota/city-rankings/most-polluted-cities.html.

Anas, A. and R. Lindsey (2011) Reducing urban road transportation externalities: road pricing in theory and in practice. *Review of Environmental Economics and Policy* 5(1), 66-88.

Apte, J.S., J.D. Marshall, A.J. Cohen, and M. Brauer (2015) Addressing global mortality from ambient $PM_{2.5}$. *Environmental Science and Technology* 49, 8057-8066.

Arnott, R. and M. Kraus (1998) When are anonymous congestion charges consistent with marginal cost pricing? *Journal of Public Economics* 67(1), 45-64.

Bachmann, J. (2007) Will the circle be unbroken: a history of the U.S. National Ambient Air Quality Standards. *Journal of the Air and Waste Management Association* 57, 652-697.

Bento, A.M., L.H. Goulder, M.R. Jacobsen, and R.H. von Haefen (2009) Disbributional and efficiency impacts of US gasoline taxes. *American Economic Review* 99(3), 667-699.

Brock, W.A. and J.A. Scheinkman (1976), Global asymptotic stability of optimal control systems with applications to the theory of economic growth. *Journal of Economic Theory* 12(1), 164-190.

Bureau of Labor Statistics (BLS) (2018) *CPI Inflation Calculator*. Available on the Internet at https://data.bls.gov/cgi-bin/cpicalc.pl.

Broome, R.A., N. Fann, T.J. Cristina, C. Fulcher, H. Duc, and G.G. Morgan (2015) The health benefits of reducing air polution in Sydney Australia. *Environmental Research* 143 (A), 19-25.

Burtraw, D., A.J. Krupnick, E. Mansur, D. Austin, and D. Farrell (1998) The costs and benefits of reducing air pollutants related to acid rain. *Contemporary Economic Policy* 16, 379-400.

Button, K. and E. Verhoef (1998) *Road Pricing, Traffic Congestion, and The Environment*. Edward Elgar Publishing: Northhampton, MA.

Caiazzo, F., A. Ashok, I.A. Waitz, S.H.L Yim, S.R.H. Barrett (2013) Air pollution and early deaths in the United States. Part 1: Quantifying the impact of major sectors in 2005. Atmospheric Environment 79, 198-208.

Cameron, C.A. and P.K. Trivedi (2005), *Microeconometrics: Methods and Applications*. Cambridge, UK: Cambridge University Press, pp. 137-139.

California Governor's Office (CGO) (2016) ZEV action plan: an updated roadmap toward 1.5 million zero-emission vehicles on California roadways by 2025. *Governor's Interagency Working Group Report on Zero-Emission Vehicles*. Available on the internet at https://www.gov.ca.gov/wp-content/uploads/2017/09/2016 ZEV Action Plan.pdf.

Chen Y, G.Z. Jin, N. Kumar, and G. Shi (2013), The promise of Beijing: evaluating the impact of the 2008 Olympic games on air quality. *Journal of Environmental Economics and Management* 66, 424443.

Chiang, A.C. (1992), *Elements of Dynamic Optimization*. New York: McGraw-Hill, Inc.

Chiang, A.C. and K. Wainwright (2005), *Fundamental Methods of Mathematical Economics*, Fourth Edition. New York: McGraw-Hill Higher Education.

Cropper, M. L., Y. Jiang, A. Alberini, A., and P. Baur (2014) Getting cars off the road: the cost effectiveness of an episodic pollution control program. *Environmental and Resource Economics* 57, 117-143.

Cumby, R. and J. Huizinga (1992) Testing the autocorrelation structure of disturbances in ordinary least squares and instrumental variables regressions. *Econometrica* 60(1), 185-195.

Cummings, R.G. and M.B. Walker (2000) Measuring the effectiveness of voluntary emission reduction programmes. *Applied Economics* 32(13), 1719-1726.

Cutter, W.B. and M. Neidell (2009) Voluntary information programs and environmental regulation: evidence from Spare the Air. *Journal of Environmental Economics and Management* 58(3), 253-265.

Davidson, R. and J.G. MacKinnon (1993) *Estimation and Inference in Econometrics* New York: Oxford University Press.

Dockery, D.W., C.A. Pope III, X. Xu, J.D. Spengler, J.H. Ware, M.E. Fay, B.G. Ferris, and F.A. Speizer (1993) An association between air pollution and mortality in six U.S. cities. *The New England Journal of Medicine* 329(24), 1753-1759.

Durbin, J. (1970) Testing for serial correlation in least-squares regressions when some of the regressors are lagged dependent variables. *Econometrica* 38, 410421.

Environmental Public Health Tracking Program (EPHCP) (2017) Air Pollution and Public Health in Utah. Available on the internet at http://health.utah.gov/enviroepi/healthyhomes/epht/AirPollution PublicHealth.pdf.

Eskeland, G. (1994) A presumptive Pigovian tax: complementing regulation to mimic an emissions fee. *World Bank Economic Review* 3(3), 373-394.

Fullerton, D. and S.E. West (2002) Can taxes on cars and on gasoline mimic an unavailable tax on emissions? *Journal of Environmental Economics and Management* 43, 135-157.

Fullerton, D. and S.E. West (2010) Tax and subsidy combinations for the control of car pollution. *The B.E. Journal of Economic Analysis and Policy* 10(1), ISSN (Online) 1935-1682.

Gallego F, J.P. Montero and C. Salas (2013a), The effect of transport policies on car use: a bundling model with applications. *Energy Economics* 40, S85S97.

Gallego F, J.P. Montero and C. Salas (2013a), The effect of transport policies on car use: evidence from Latin American cities. *Journal of Public Economics* 107, 4762.

Green Auto Market (GAM) (2016) What studies are finding: adoption of clean vehicle technologies will stay small-scale for now but we're likely approaching the cusp of change. Available on the internet at http://greenautomarket.com/studies-finding-adoption-clean-vehicle-technologies-will-stay-small-scale-now-likely-approaching-cusp-change/.

Greenstone, M., E. Kopits, and A. Wolverton (2013) Developing a social cost of carbon for US regulatory analysis: a methodology and interpretation. *Review of Environmental Economics and Policy* 7(1), 23-46.

Hamada, M. and C.F.J. Wu (1992) Analysis of designed experiments with complex aliasing. *Journal of Quality Technology* 24, 130-137.

Harrington, W., V. McConnell, and A. Alberini (1998) Economic incentive policies under uncertainty: the case of vehicle emission fees, in *Environment and Transport in Economic Modeling* (R. Roson and K. A. Small, Eds.), Kluwer Academic, Dordrecht.

Henry, G.T. and C.S. Gordon (2003) Driving less for better air: impacts of a public information campaign. *Journal of Policy Analysis and Management* 22(1), 45-63.

International Economic Development Council (IEDC) (2013) Creating the clean energy economy: analysis of the electric vehicle industry. Available on the internet at https://www.iedconline.org/clientuploads/Downloads/edrp/IEDC Electric Vehicle Industry.pdf.

Innes, R. (1996) Regulating automobile pollution under certainty, competition, and imperfect information, *Journal of Environmental Economics and Management* 31, 219-239.

Karagulian, F., C.A. Belis, C.F.C. Dora, A.M. Prüss-Ustün, S. Bonjour, H. Adair-Rohani, and M. Amann (2015) Contributions to cities' ambient particulate matter (PM): a systematic review of local source contributions at global level. *Atmospheric Environment* 120, 475-483.

Li, X., N. Sudarsanam, and D.D. Frey (2006) Regularities in data from factorial experiments. *Complexity* 11(5), 32-45.

Liu, B-C and E. S-H Yu (1976) *Physical and Economic Damage Functions for Air Pollutants by Receptor*. Corvallis Environmental Research Laboratory, Office of Development and Research, USEPA. EPA-600/5-76-011.

Malek, E., T. Davis, R.S. Martin, and P.J. Silva (2006) Meteorological and environmental aspects of one of the worst national air pollution episodes (January, 2004) in Logan, Cache Valley, Utah, USA. *Atmospheric Research* 79(2), 108-122.

McCubbin, D.R. and M.A. Delucchi (1999) The health costs of motor-vehicle-related air pollution. *Journal of Transport Economics and Policy* 33, 253-286.

Moscardini, L.A., and A.J. Caplan (2017) Controlling episodic air pollution with a seasonal gas tax: the case of Cache Valley, Utah. *Environmental and Resource Economics* 66(4), 689-715.

Office of Management and Budget (OMB) (2003) *Circular A-4: Regulatory Analysis*. September. Available on the internet at https://georgewbush-whitehouse.archives.gov/omb/circulars/a004/a-4.html.

Osakwe, R. (2010) An analysis of the driving restriction implemented in San Jos, Costa Rica. *Environment for Development (EfD) Policy Brief*. Available on the internet at http://www.efdinitiative.org/publications/analysis-driving-restriction-implemented-san-jose-costa-rica.

Parry, I.W.H. and K.A. Small (2005) Does Britain or the United States have the right gasoline tax? *American Economic Review* 95(4), 1276-1289.

Phaneuf, D.J. and T. Requate (2017), *A Course in Environmental Economics: Theory, Policy, and Practice*. Cambridge, UK: Cambridge University Press.

Phang, S-Y and R.S. Toh (2004) Road congestion pricing in Singapore: 1975 to 2003. *Transportation Journal* 43 (2), 16-25.

Pope, C.A., III. (1989) Respiratory disease associated with community air pollution and a steel mill, Utah Valley. *American Journal of Public Health* 79(5), 623-628.

Pope, C.A., III, M.J. Thun, M.M. Namboodiri, D.W. Dockery, J.S. Evans, F.E. Speizer, and J.C.W. Heath (1995) Particulate air pollution as a predictor of mortality in a prospective study of U.S. adults. *American Journal of Respiratory and Critical Care Medicine* 151(3pt1), 669-674.

Pope, C.A., III, R.T. Burnett, M.J. Thun, E.E. Calle, D. Krewski, K. Ito, and G.D. Thurston (2002) Lung cancer, cardiopulmonary mortality, and long-term exposure to fine particulate air pollution. *Journal of the American Medical Association (JAMA)* 287(9), 1132-1141.

Sevigny, M. (1998) *Taxing Automobile Emissions for Pollution Control*, Elgar, Cheltenham, UK.

Small, K.A. and C. Kazimi (1995) On the cost of air pollution from motor vehicles. *Journal of Transport Economics and Policy* 29, 7-32.

US Environmental Protection Agency (USEPA) (2016) Particle pollution and your health. Available on the internet at https://www.airnow.gov/index.cfm?action=particle health.index.

US Environmental Protection Agency (USEPA) (2017), *Nonattainment Areas for Criteria Pollutants (Green Book)*. Available on the internet at https://www.epa.gov/green-book.

US Environmental Protection Agency (USEPA) (2018), *Environmental Benefits Mapping and Analysis Program (BenMAP)- Community Edition*, version 1.3.7.1. Research Triangle Park, NC. Available on the internet at http://www.epa.gov/benmap/.

US Federal Highway Administration (USFHWA) (2000) *Addendum to the 1997 Federal Highway Cost Allocation Study Final Report*. US Department of Transportation, Washington DC.

Utah Air Quality Board (UAQB) (2014) *Utah State Implementation Plan: Control Measures for Area and Point Sources, Fine Particulate Matter, PM$_{2.5}$ SIP for the Logan, UT-ID Nonattainment Area* Section IX. Part A.23. Available on the internet at https://deq.utah.gov/legacy/laws-and-rules/air-quality/sip/docs/2014/12Dec/SIP20IX.A.23 Logan FINAL Adopted12-3-2014.pdf.

Utah Climate Center (2016) *Climate GIS—Station(s)*. Available on the internet at https://climate.usurf.usu.edu/mapGUI/mapGUI.php.

Utah Department of Environment Quality (UDEQ) (2016a) *Particulate Matter*. Available on the internet at http://www.deq.utah.gov/Pollutants/P/pm/Inversion.htm.

Utah Department of Environment Quality (UDEQ) (2016b) Information Sheet, p. 2. Available on the internet at http://www.deq.utah.gov/Topics/FactSheets/docs/handouts/pm25sipfs.pdf

Utah Department of Environment Quality (UDEQ) (2016c) *Utah Air Monitoring Program*. Available on the internet at http://www.airmonitoring.utah.gov/network/Counties.htm

Utah Department of Transportation (UDOT) (2014) *Traffic statistics* Available on the internet at http://www.udot.utah.gov/main/f?p=100:pg::::1:T,V:507.

Utah State Tax Commission (USTC) (2018) *Utah Vehicle Registrations*. Available on the internet at https://tax.utah.gov/econstats/mv/registration.

Wang, S.-Y., L.E. Hipps, O.-Y. Chung, R.R. Gillies, and R. Martin (2015) Long-term winter inversion properties in a mountain valley of the western United States and implications on air quality. *Journal of Applied Meteorology and Climatology* 54, 2339-2352.

Weather Underground (2016) *About Our Data*. Available on the internet at http://www.wunderground.com/about/data.asp.

West, S.E. and R.C. Williams III (2005) The cost of reducing gasoline consumption. *American Economic Review* 95(2), Papers and Proceedings of the One Hundred Seventeenth Annual Meeting of the American Economic Association, 294-299.

World Health Organization (WHO) (2006) WHO air quality guidelines for particulate matter, ozone, nitrogen dioxide and sulfur dioxide. *Global Update 2005*, Summary of Risk Assessment. Geneva, Switzerland: WHO Press.

World Health Organization (WHO) (2017) *Media Center*. Available on the internet at http://www.who.int/mediacentre/news/releases/2016/air-pollution-estimates/en/.

Zhang, W., C-Y.C.L. Lawell, and V.I. Umanskaya (2016), The effects of license plate-based driving restrictions on air quality: theory and empirical evidence. Unpublished manuscript, University of California at Davis. Available at http://www.des.ucdavis.edu/faculty/Lin/driving_ban_paper.pdf.

Figure 1: Phase diagram for steady-state equilibrium.
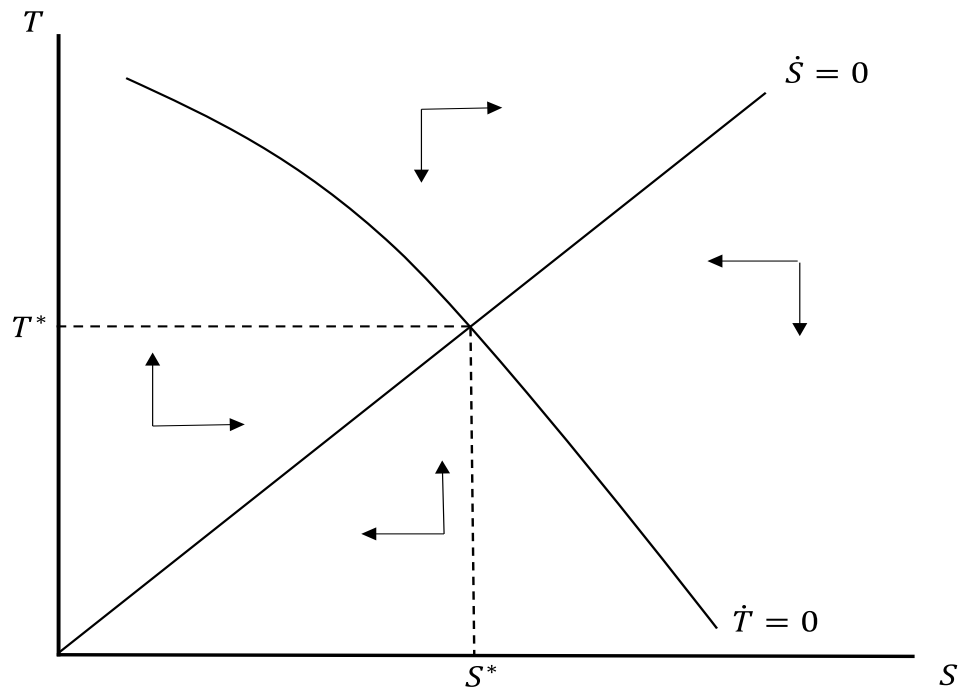
Figure 2: Northern Utah, Cache County.
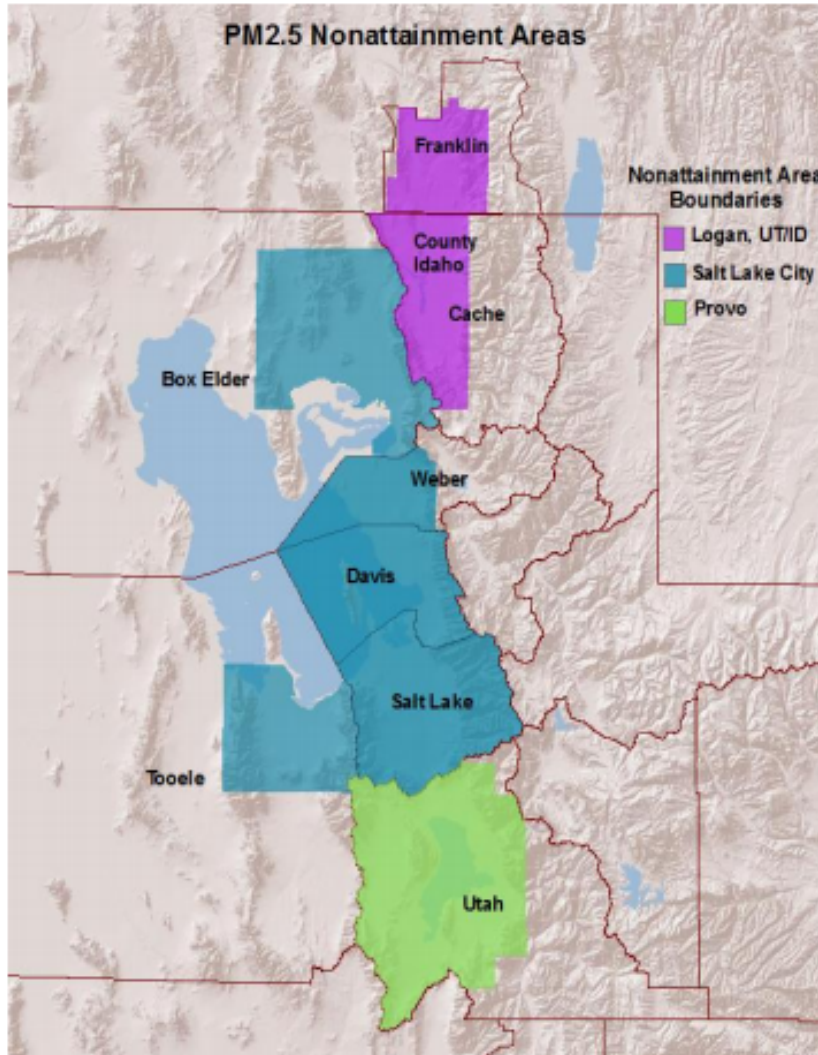
Figure 3: Annual $PM_{2.5}$ concentrations in Cache Valley, Utah, 2002 2007.
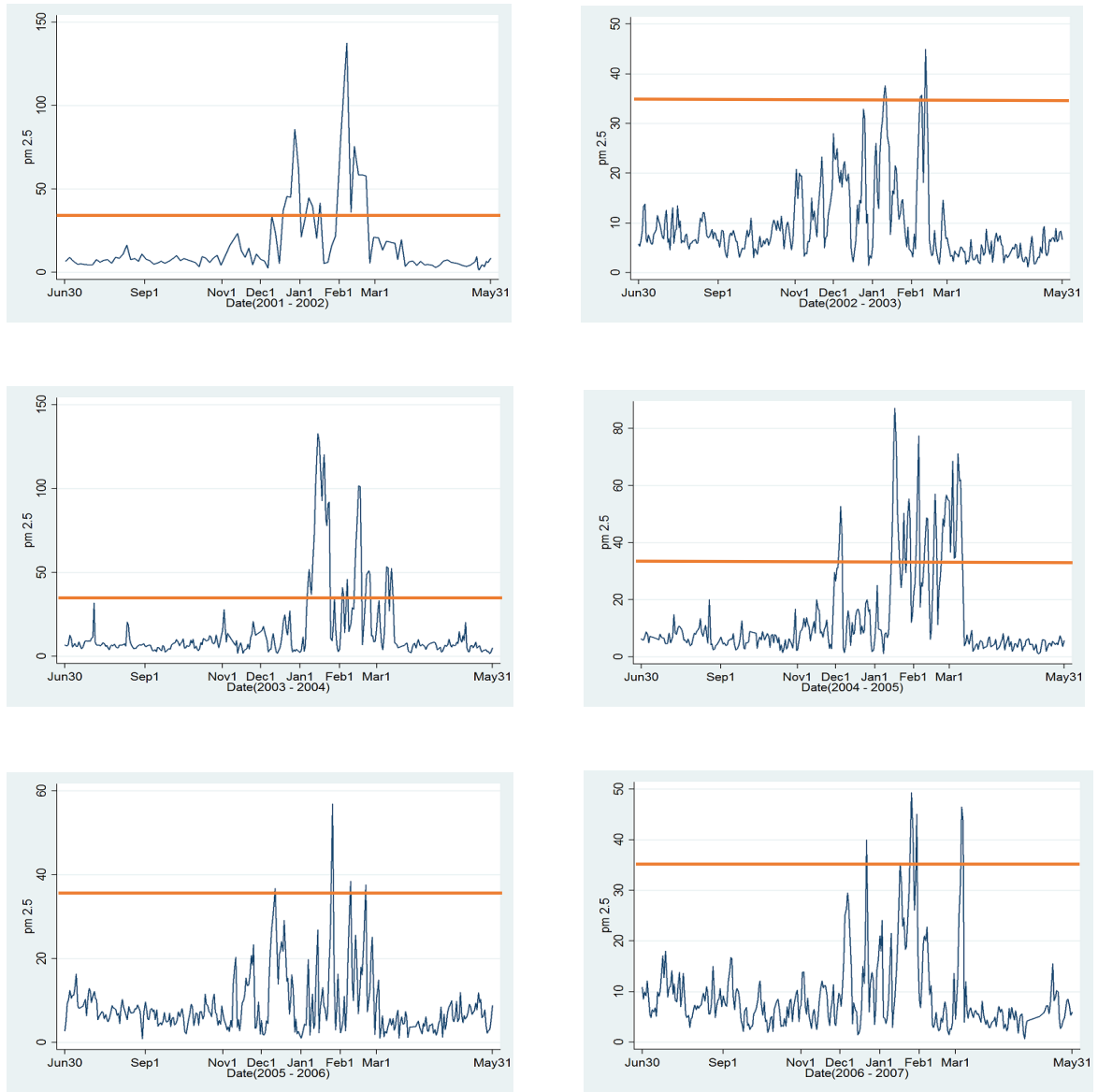
Figure 4: Coincidence of $PM_{2.5}$ concentrations and temperature inversion, January 2004.
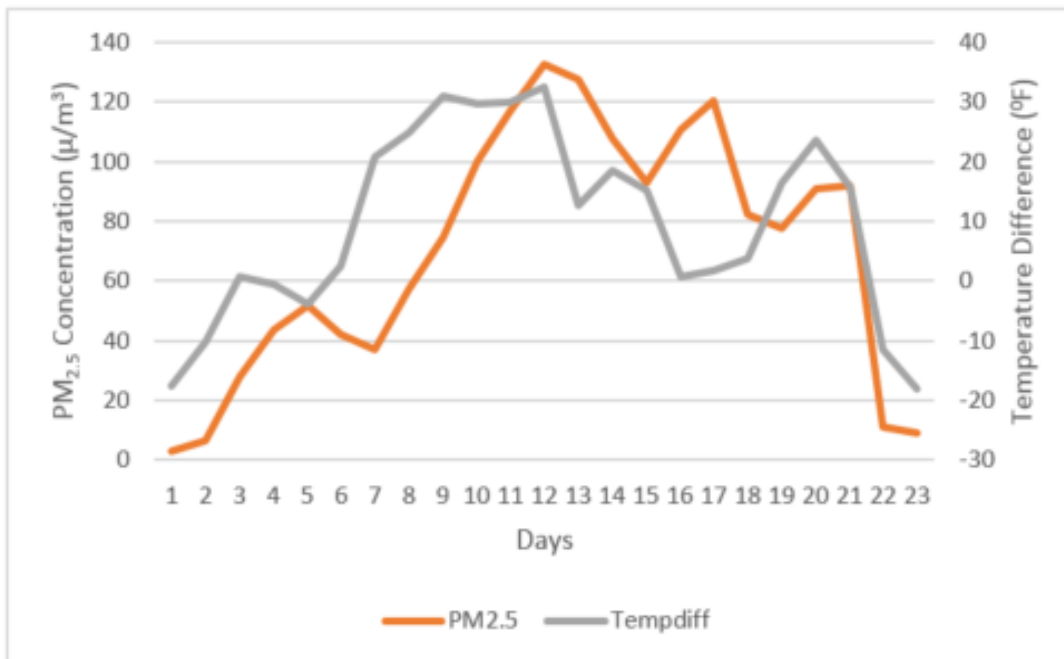
Figure 5: Damage function.
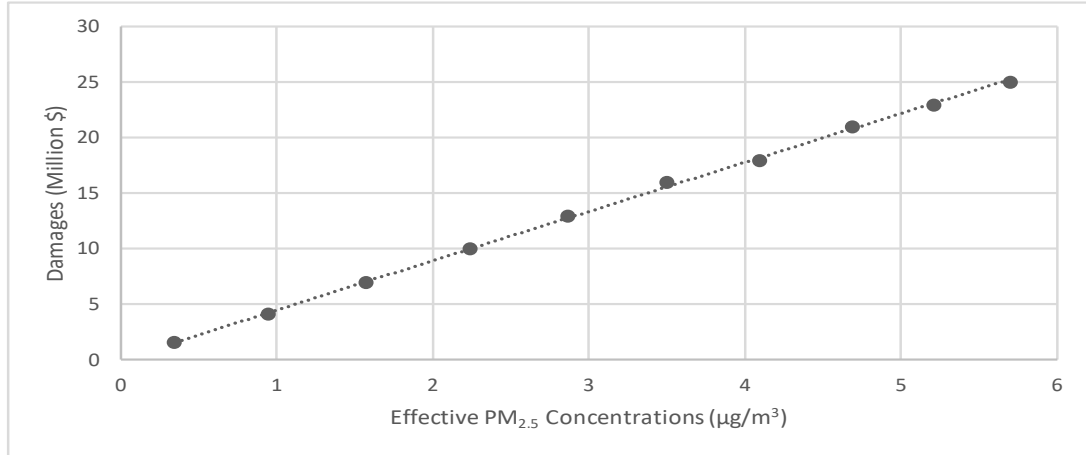
Figure 6: Optimal time path for vehicle trip counts.
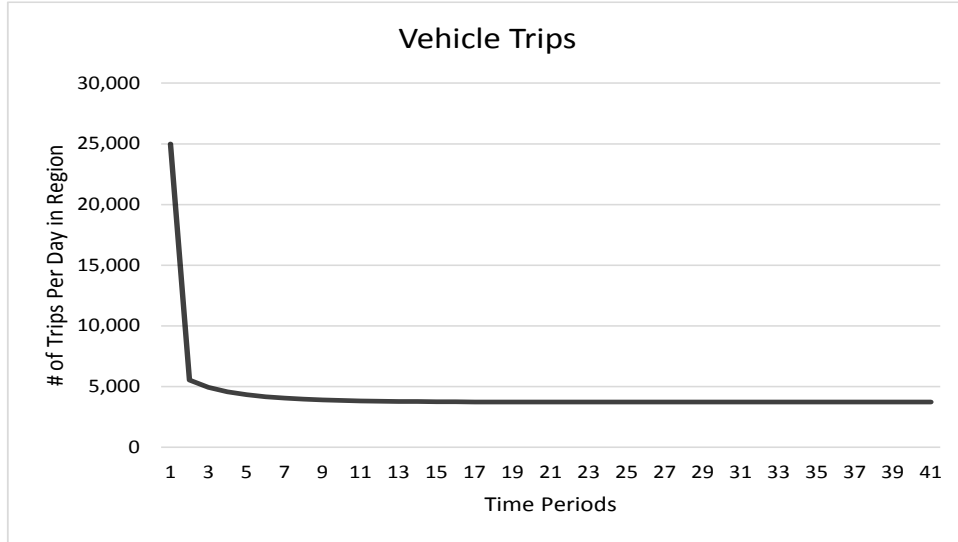
Figure 7: Optimal time path for $PM_{2.5}$ concentration levels.

PM2.5 Concentrations
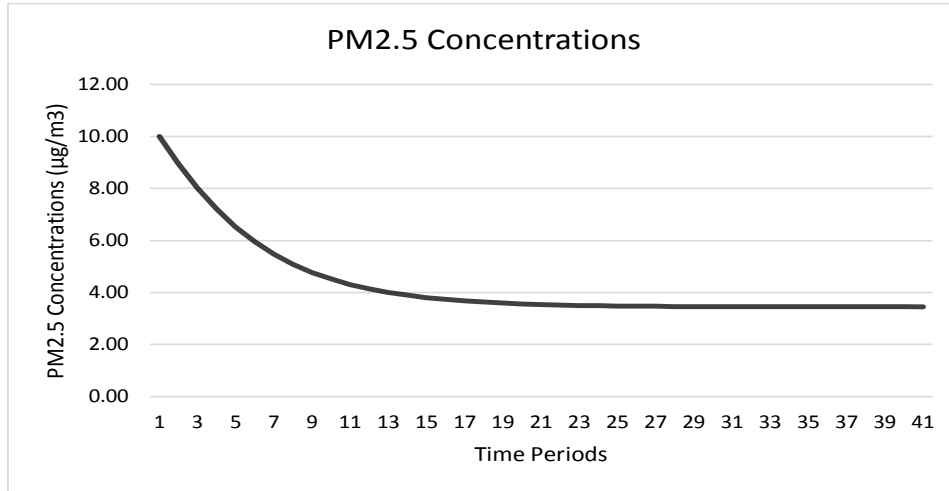
Figure 8: Optimal time path for vehicle trip counts $(B(T) = b\ln(T))$.

Vehicle Trips
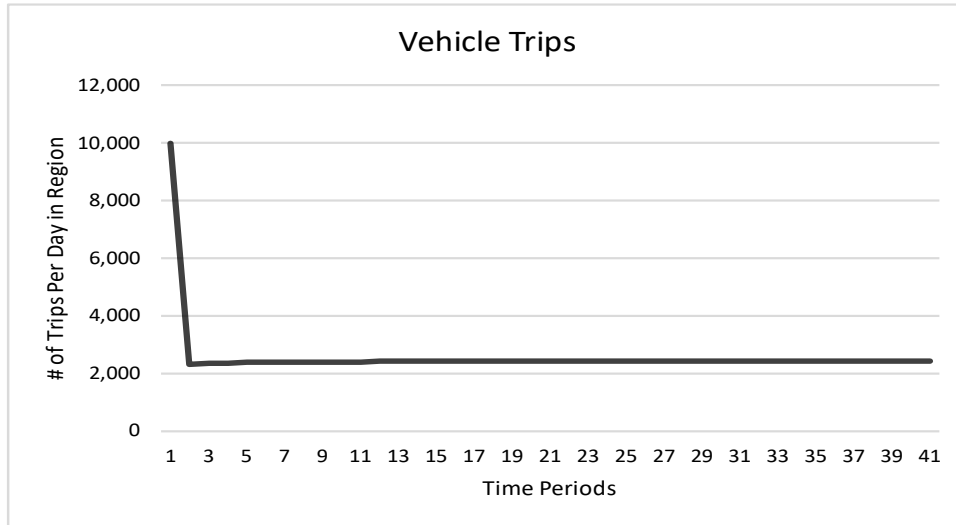
Figure 9: Optimal time path for $PM_{2.5}$ concentration levels $(B(T) = b\ln(T))$.

PM2.5 Concentrations

PM2.5 Concentrations (µg/m3) vs *Time Peiods*
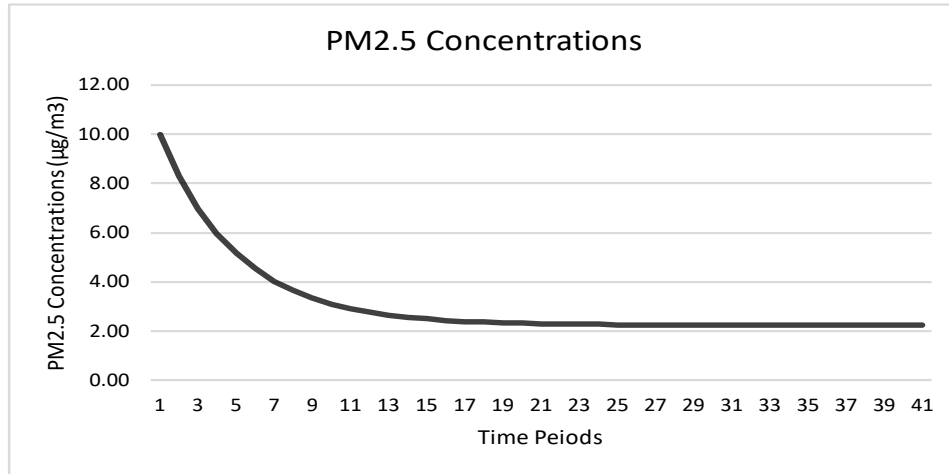
Table 1: Red air day episodes (RADEs) and temperature inversion events (TIEs), Cache County, Utah.

Year	#RADE	RADE Length (Days)	#TIE	TIE Length (Days)	Rel. Freq (%)
2003	2	5.33	2	2.50	16.67
2004	7	7.71	3	8.00	36.54
2005	8	6.50	6	4.83	40.38
2006	4	4.50	4	2.25	24.53
2007	3	5.67	3	3.67	17.78
2008	4	4.50	5	2.60	17.78
2009	6	6.00	6	3.33	36.96
2010	7	4.71	5	2.40	23.68
2011	2	7.50	4	3.25	18.75
2012	0	0	3	2.00	9.09
Average	4.3	5.24	5.5	3.48	24.23

Table 2: Variable definitions and summary statistics.

Variable	Description	Mean (SD)*
$\dot{S}$	Change in (mean) daily $PM_{2.5}$ concentration level ($\mu g/m^3$), i.e., $S_t - S_{t-1}$.	-0.06 (10.42)
S	Daily (mean) $PM_{2.5}$ concentration ($\mu g/m^3$), i.e., S_t.	18.22 (18.52)
T	Daily trip count (# vehicle trips).	44,997 (14,922)
$TEMP$	Temperature gradient between Logan Peak and valley floor ($^\circ F$).	-8.15 (9.70)
$TEMP_{|TEMP>0}$	Temperature gradient given gradient is larger than zero ($^\circ F$).	8.74 (7.90)
$S_{|TEMP>0}$	Daily $PM_{2.5}$ concentration given gradient is larger than zero ($\mu g/m^3$).	37.03 (28.69)
HUM	Daily humidity level (%).	81.90 (8.82)
$WIND$	Daily wind speed (miles/hour).	3.12 (2.68)
$HUMWIND$	$HUM*WIND$.	249.41 (203.99)
$SNOWF$	Daily snowfall level (mm).	14.22 (36.14)
$SNOWD$	Daily snow depth (mm).	123.65 (110.76)
$PRESS$	Daily atmospheric pressure (p.s.i.).	30.18 (0.27)

* Overall mean (Mean) and associated standard deviation (SD). Sample sizes for respective variables range between 131 for $TEMP_{|TEMP>0}$ and 810 for HUM and $WIND$.

Table 3: Regression results (dependent variable $\dot{S}$).[a]

Explanatory Variables	Model 1	Model 2
CONSTANT	132.00	-9.33
	(232.41)	(10.04)
$\dot{S}_{t-1}$	0.22***	0.22***
	(0.05)	(0.05)
$\dot{S}_{t-2}$	-0.05	-0.06
	(0.04)	(0.04)
S_{t-1}	-6.14	-5.99
	(7.90)	(6.49)
T	0.0008	0.004**
	(0.003)	(0.002)
$YEAR$	-0.28*	-0.26*
	(0.15)	(0.16)
HUM	0.20**	0.23*
	(0.13)	(0.13)
$HUMWIND$	-0.01	-0.009**
	(0.007)	(0.004)
$SNOWF$	-0.04	-0.03
	(0.03)	(0.03)
$SNOWD$	0.02*	0.02*
	(0.01)	(0.01)
$PRESS$	-4.67	—
	(7.63)	
$S_{t-1}*HUMWIND$	-0.0006**	-0.0006**
	(0.0003)	(0.0003)
$S_{t-1}*SNOWF$	-0.004***	-0.004***
	(0.001)	(0.001)
$T*TEMP$	0.0003*	0.0003***
	(0.0001)	(0.0001)
$T*HUMWIND$	2.8e-07*	1.3e-07
	(1.7e-07)	(8.6e-08)
$T*PRESS$	-0.00002	-0.0001*
	(0.0001)	(0.00007)
$T*HUMWIND*TEMP$	3.0e-08*	—
	(1.6e-08)	
$T*SNOWF*TEMP$	-1.1e-07***	-9.6e-08***
	(3.2e-08)	(3.0e-08)
$T*SNOWD*TEMP$	3.9e-08***	3.8e-08***
	(1.3e-08)	(1.3e-08)
$T*PRESS*TEMP$	-9.1e-06**	-0.00001***
	(4.6e-06)	(3.5e-06)
$F(27,378)$	28.33***	31.32***
R^2	0.65	0.64
$Durbin\chi^2$	0.04	0.03
N	406	406

a Robust standard errors in parentheses (Cameron and Trivedi, 2005). *** Significant at 1% level, ** Significant at 5% level, * Significant at 10% level.

Table 4: Estimates of β_T and β_S.

Coefficients	Model 1	Model 2
β_T	0.0001989	0.0002545
β_S	-0.2146	-0.2004

Table 5: Estimates of T^* (#trips), S^* ($\mu g/m^3$), and λ^* ($1,000).

Variables	Model 1	Model 2
$r = 0.01$		
T^*	3,138	1,682
S^*	2.91	2.14
λ^*	$220	$234
$r = 0.03$		
T^*	3,722	2,017
S^*	3.45	2.56
λ^*	$202	$214
$r = 0.05$		
T^*	4,356	2,383
S^*	4.04	3.03
λ^*	$186	$197
$r = 0.07$		
T^*	5,039	2,778
S^*	4.67	3.53
λ^*	$202	$214

Table 6: Estimates of T^* (#trips), S^* ($\mu g/m^3$), and λ^* ($1,000) ($B(T) = b\ln(T)$).

Variables	Model 1	Model 2
$r = 0.01$		
T^*	2,218	1,624
S^*	2.06	2.06
λ^*	$220	$234
$r = 0.03$		
T^*	2,416	1,778
S^*	2.24	2.26
λ^*	$202	$214
$r = 0.05$		
T^*	2,613	1,933
S^*	2.42	2.45
λ^*	$186	$197
$r = 0.07$		
T^*	2,811	2,087
S^*	2.61	2.65
λ^*	$202	$214